Thermodynamics and mechanics of stretch-induced crystallization in rubbers

Qiang Guo,[1,2] Fahmi Zaïri,[1,*] and Xinglin Guo[2]
[1]*Lille University, Civil Engineering and geo-Environmental Laboratory (EA 4515 LGCgE), 59000 Lille, France*
[2]*Dalian University of Technology, Department of Engineering Mechanics, 116024 Dalian, China*

(Received 17 January 2018; published 22 May 2018)

The aim of the present paper is to provide a quantitative prediction of the stretch-induced crystallization in natural rubber, the exclusive reason for its history-dependent thermomechanical features. A constitutive model based on a micromechanism inspired molecular chain approach is formulated within the context of the thermodynamic framework. The molecular configuration of the partially crystallized single chain is analyzed and calculated by means of some statistical mechanical methods. The random thermal oscillation of the crystal orientation, considered as a continuous random variable, is treated by means of a representative angle. The physical expression of the chain free energy is derived according to a two-step strategy by separating crystallization and stretching. This strategy ensures that the stretch-induced part of the thermodynamic crystallization force is null at the initial instant and allows, without any additional constraint, the formulation of a simple linear relationship for the crystallinity evolution law. The model contains very few physically interpretable material constants to simulate the complex mechanism: two chain-scale constants, one crystallinity kinetics constant, three thermodynamic constants related to the newly formed crystallites, and a function controlling the crystal orientation with respect to the chain. The model is used to discuss some important aspects of the micromechanism and the macroresponse under the equilibrium state and the nonequilibrium state involved during stretching and recovery, and continuous relaxation.

DOI: 10.1103/PhysRevE.97.052501

I. INTRODUCTION

Firstly observed in 1925 by Katz [1], the stretch-induced crystallization in natural rubber has a long research history. Although it also concerns synthetic rubbers, it is now well recognized that the ability of this biopolymer to crystallize under stretching is mainly due to the highly regular macromolecular structure. The transformation of the chain from its amorphous to crystalline state can be understood from the thermodynamic viewpoint. When the chain is stretched from its most probable conformation, its alignment results in a decrease in the conformational entropy. Thus, less entropy is needed to be sacrificed in the transformation of the chain from its amorphous to crystalline state. Due to this decrease in total entropy of fusion, the stretch-induced crystallization is allowed to occur at higher temperatures than under quiescent conditions. The process of stretch-induced crystallization has a depth impact on the mechanical properties, and in particular, it contributes to superior fatigue properties and crack growth resistance [2–4] as well as history-dependent mechanical features such as hysteretic effects [5–13] and continuous relaxation [14–17]. There are considerable qualitative experimental observations on the stretch-induced crystallization in natural rubber, as reported in recent literature reviews [18–20], but the quantitative predictive modeling of this fascinating phenomenon is far from being fully established and remains a challenging task.

A predictive constitutive theory is, indeed, fundamental to better understanding the relationship between the thermomechanical response at the macroscale and the stretch-induced crystallization at the microscale, for which numerous phenomena accompanying the material transformation are still misunderstood. A literature survey shows that there exist only five recent contributions dealing with this task in rubbers [21–26] and all the proposed constitutive models can be distinguished by the restrictive assumptions, the theoretical approach, and the predictive capabilities. The development of a rigorous physically based predictive model of this mechanism has to take into account, within the context of the thermodynamic framework, the particular chain configuration by means of the statistical mechanics. In this regard, three main aspects have to be taken into account such as (i) the definition of a pertinent single chain configuration that can be then translated to the chain network, (ii) the derivation of the chain free energy becoming that of the chain network, and (iii) the proposition of an appropriate crystallization kinetics and its evolution law. The second point is the key element in the thermodynamic formulation of the constitutive relations between various thermodynamic quantities, and is related to the microstructural specificities of the rubber gum by means of the first point. The third point introduces into the constitutive relationships the microstructural evolution using either a purely phenomenological evolution law or a more physically realistic evolution law, its physical consistency allowing especially to limit the number of parameters with no direct physical meaning.

The stretch-induced crystallization in a rubber chain was investigated, using the statistical mechanics and within the thermodynamic framework, for the first time in 1947 by Flory in his early work [27]. In his theory, bounded by several simplifying assumptions, Flory [27,28] considered that the final partially crystallized chain is achieved from an initially

*Corresponding author: fahmi.zairi@polytech-lille.fr

fully amorphous chain by two separate and distinct steps, namely, stretching and crystallization, and the crystallized part in the chain was assumed to be fully extended and oriented in the stretching direction. The Flory [27,28] theory predicts the equilibrium crystallization as a function of stretch and temperature, and was verified with experimental observations [29,30]. Later, other models based on the Flory [27,28] theory were proposed by eliminating some assumptions. Roe *et al.* [31], Gaylord [32] and Gaylord and Lohse [33] considered the crystallite morphology in crystallized polymer chains whereas Smith [34] took into account the orientation of the extended crystallized part with respect to the chain. In the previous models, the crystallization occurs in a thermodynamically most favorable condition, i.e., in a thermodynamic equilibrium condition. Since this equilibrium crystallization is assumed without time evolution and achieved only under infinitesimal change rates, it is necessary to extend the theory to nonequilibrium conditions where the crystallinity evolution should be described in a certain kinetics theory.[1] Different descriptions of the crystallization kinetics were proposed in the five recent contributions [21–26]. Kroon [21] proposed a model by defining the crystallinity degree as the fraction of the partially crystallized chains with fixed-size nucleated crystallites without crystallite growth. In his model, the contribution of the crystallites to the free energy is neglected and a phenomenological Arrhenius-type kinetics is introduced to govern the crystallinity evolution. Dargazany *et al.* [22,23] also took the crystallite size in a single chain as a material constant whereas the crystallinity evolution law was formulated on the basis of the chain length statistic distribution. Mistry and Govindjee [24] proposed a model in which the free energy is considered to only consist of a purely thermodynamic part and an elastic part. In their model, the crystallization kinetics is formulated based on the free energy gradient with respect to the crystallinity degree, and a yieldlike threshold is introduced to additionally restrict the evolution law. Guilie *et al.* [25] also related the crystallization kinetics with the free energy gradient, but they formulated the evolution law using a plasticlike flow rule and made a distinction between the processes of crystallization and melting. Very recently, Rastak and Linder [26] derived the chain free energy by integrating the chain force with respect to the chain length and adding an integration constant only dependent on the crystallinity degree. In their approach, a linear relationship between the free energy gradient and the crystallization rate was directly adopted to capture the rate-dependent crystallinity evolution.

In this contribution, we present a new micromechanism inspired molecular chain model to describe the progressive evolution of the crystallinity degree in rubbers and the history-dependent thermomechanical response within the context of the thermodynamic framework. In our model, the orientation of the crystallization domain with respect to the chain is considered as a continuous random variable which is treated by means of a representative angle. In the spirit of the Flory [27,28] theory, we derive the chain free energy via a two-step strategy by separating crystallization and stretching. Although hypothetical, the method allows us to derive a physically realistic model insuring that the free energy gradient, used to formulate the crystallinity evolution law, is null at the initial state under the melting temperature, ignoring the crystallite surface energy. The method avoids the introduction of any additional constraint to describe the progressive evolution of the crystallinity degree which obeys a linear relationship between the crystallization rate and the corresponding thermodynamic force.

The outline of the present paper is as follows. We give the main elements of the developed model in Sec. II. Section III presents and discusses the model results. Concluding remarks are finally given in Sec. IV.

II. THEORY

Let us consider a single chain with a total number of N segments each of length l, for a fully extended chain length of Nl. During the crystallization, a portion of the molecular chain crystallizes while the remaining part remains amorphous as illustrated in Fig. 1. The two amorphous subparts are present from either side of the crystallized portion, and are assumed to not interact and to have a random distribution. We confer the subscript 1 to the left amorphous subpart and the subscript 2 to the right amorphous subpart. The conservation of the total number of segments leads to

$$N = N_{\mathrm{c}} + N_{\mathrm{a\_1}} + N_{\mathrm{a\_2}}, \tag{1}$$

where N_{c} is the number of crystallized segments and $N_{\mathrm{a}} = N_{\mathrm{a\_1}} + N_{\mathrm{a\_2}}$ is the total number of amorphous segments:

$$N_{\mathrm{a}} = N(1-\chi), \tag{2}$$

in which $\chi \in [0,1]$ is the crystal fraction in the single chain given by the following ratio[2]:

$$\chi = \frac{N_{\mathrm{c}}}{N}. \tag{3}$$

The chain end-to-end vector $\boldsymbol{r}$ is the sum of three parts:

$$\boldsymbol{r} = \boldsymbol{r}_{\mathrm{c}} + \boldsymbol{r}_{\mathrm{a\_1}} + \boldsymbol{r}_{\mathrm{a\_2}}, \tag{4}$$

in which $\boldsymbol{r}_{\mathrm{c}}$ is the end-to-end vector of the crystallized part and $\boldsymbol{r}_{\mathrm{a}} = \boldsymbol{r}_{\mathrm{a\_1}} + \boldsymbol{r}_{\mathrm{a\_2}}$ is the sum of the end-to-end vectors of the two amorphous subparts. Introducing $\theta \in [0,\pi]$ as the angle between $\boldsymbol{r}$ and $\boldsymbol{r}_{\mathrm{c}}$, a simple relationship between the lengths of these end-to-end vectors is given:

$$r_{\mathrm{a}} = \sqrt{r^2 + r_{\mathrm{c}}^2 - 2 r r_{\mathrm{c}} \cos\theta}, \tag{5}$$

where $r = \|\boldsymbol{r}\|$, $r_{\mathrm{c}} = \|\boldsymbol{r}_{\mathrm{c}}\|$, and $r_{\mathrm{a}} = \|\boldsymbol{r}_{\mathrm{a}}\|$.

[1]The crystallization kinetics in solids was firstly investigated by Avrami [35–37] and classical equations have emerged for spherulitic growth in thermally induced crystallization but are not useful for all kinetics of newly formed crystals due to differences in morphology and in size. As a matter of fact, the micron-sized spherulites in semicrystalline thermoplastic polymers resulting from quiescent melt crystallization are different than the newly formed nanosized crystallites in natural rubbers due to stretching.

[2]We can notice that the single chain crystallization can be generalized to define the material crystallinity degree by implementing the actual chain structure for all chains in the network. This procedure gives us a spatially averaged measure of the material crystallinity.

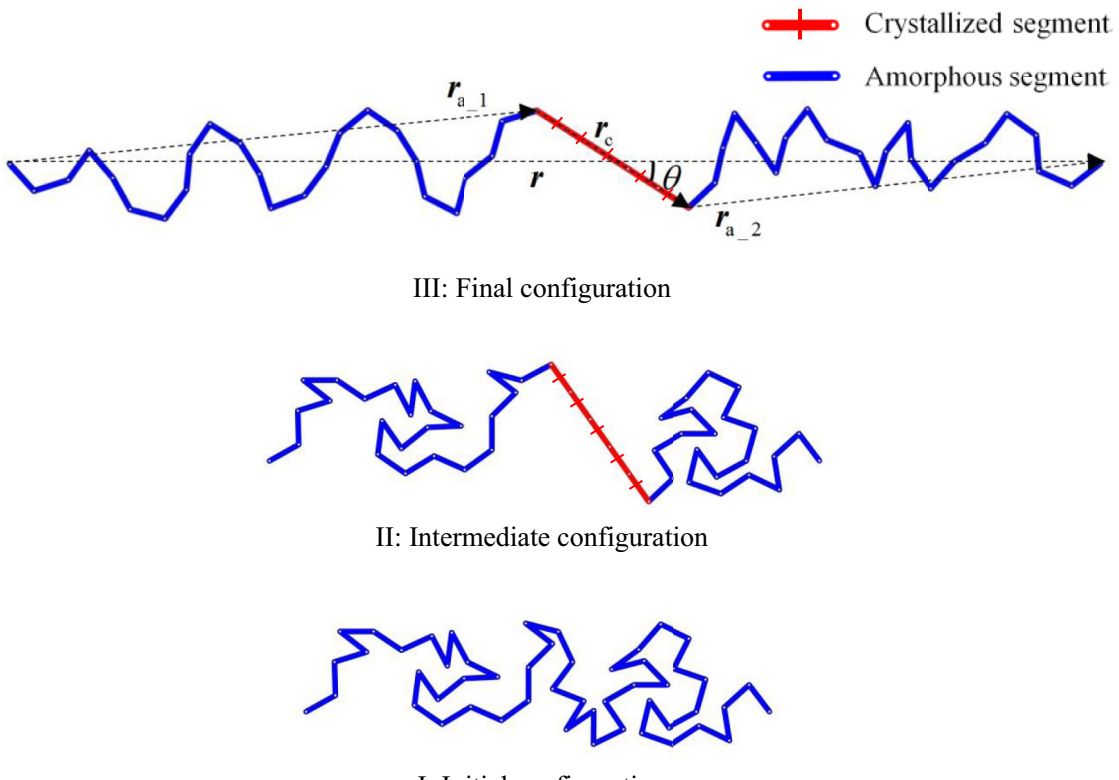

FIG. 1. Configuration changes in the proposed two-step strategy: I→II, thermal-induced crystallization step, and II→III, absolutely mechanical stretching step.

A. Configuration

As a matter of fact, the partially crystallized chain continuously oscillates due to thermal fluctuations. Owing to the internal rotation of molecular bonds, a huge number of molecular chain configurations are possible, which requires statistical mechanical methods to establish the average mechanical properties. In our micromechanism inspired molecular chain model, the configurations of the crystallized part and the two amorphous subparts are assumed to be independent from each other and, hence, the configuration of the whole chain can be identified by comprehensively analyzing the individual oscillation of the amorphous and crystallized parts.

The amorphous segments are assumed to be rotationally jointed with complete freedom of orientation and with no interaction [38]; i.e., the rotation is free at each bond junction and all bond angles take the same probability with no preferred bond angle in the absence of external forces. The non-Gaussian statistical method is used to calculate the configurations of the two amorphous subparts. Contrary to a Gaussian treatment, the non-Gaussian probability density function of the molecular chain configuration allows us to introduce the values of $r_{a\_1} = \|\boldsymbol{r}_{a\_1}\|$ and $r_{a\_2} = \|\boldsymbol{r}_{a\_2}\|$ over their whole ranges up to the fully extended lengths $N_{a\_1}l$ and $N_{a\_2}l$:

$$P_{a\_1}(\boldsymbol{r}_{a\_1}) = \left(\frac{3}{2\pi N_{a\_1}l^2}\right)^{3/2} \exp\left\{-N_{a\_1}\Re\left(\frac{r_{a\_1}}{N_{a\_1}l}\right)\right\}, \quad (6)$$

$$P_{a\_2}(\boldsymbol{r}_{a\_2}) = \left(\frac{3}{2\pi N_{a\_2}l^2}\right)^{3/2} \exp\left\{-N_{a\_2}\Re\left(\frac{r_{a\_2}}{N_{a\_2}l}\right)\right\}, \quad (7)$$

in which we define $\Re(x)$ as a function depending on the inverse function $\mathcal{L}^{-1}(x)$ of the Langevin function $\mathcal{L}(x) = \coth(x) - 1/x$:

$$\Re(x) = x\mathcal{L}^{-1}(x) + \ln\frac{\mathcal{L}^{-1}(x)}{\sinh[\mathcal{L}^{-1}(x)]}, \quad (8)$$

where the Padé approximation $\mathcal{L}^{-1}(x) \approx x(3 - x^2)/(1 - x^2)$ is used.

Considering that the two amorphous subparts have independent configurations, the probability density function of the whole amorphous part $P_a(\boldsymbol{r}_a)$ can be derived through the convolution integration $*$ of the two probability density functions $P_{a\_1}(\boldsymbol{r}_{a\_1})$ and $P_{a\_2}(\boldsymbol{r}_{a\_2})$:

$$\begin{aligned} P_a(\boldsymbol{r}_a) &= P_{a\_1}(\boldsymbol{r}_{a\_1}) * P_{a\_2}(\boldsymbol{r}_{a\_2}) \\ &= \int_{\mathbb{R}^3} P_{a\_1}(\boldsymbol{r}_{a\_1}) P_{a\_2}(\boldsymbol{r}_a - \boldsymbol{r}_{a\_1}) d\boldsymbol{r}_{a\_1} \end{aligned} \quad (9)$$

After a series of lengthy but straightforward derivations, we obtain the following expression:

$$P_a(\boldsymbol{r}_a) = \left(\frac{3}{2\pi N_a l^2}\right)^{3/2} \exp\left\{-N_a\Re\left(\frac{r_a}{N_a l}\right)\right\}. \quad (10)$$

The formula (10) points out that the probability density of the amorphous part is invariant with respect to the position of the crystallized domain inside the single chain. In other words, all the possible configurations of the amorphous segments have been taken into account including those induced by the various possible partitions of each amorphous subpart.

In the absence of external forces, the most probable end-to-end distance of the amorphous part r_a, according to Eq. (10), has the root mean square value $l\sqrt{N_a}$. Thus, a kinematic variable λ_a of the amorphous part can be introduced through the effective stretch definition:

$$\lambda_a = \frac{r_a}{l\sqrt{N_a}}. \tag{11}$$

Similarly, with regard to the partially crystallized chain, the whole stretch λ can be defined as

$$\lambda = \frac{r}{l\sqrt{N}}. \tag{12}$$

In our micromechanism inspired molecular chain model, the crystallized part is considered as a rigid entity with fully extended segments and its length r_c is identically equal to the algebraic sum of the length of N_c crystallized segments:

$$r_c = N_c l. \tag{13}$$

Moreover, the configuration of the crystallized part may be characterized by the angle θ between $\boldsymbol{r}$ and $\boldsymbol{r}_c$. Due to the thermal fluctuations, this angle is in nature a continuous random variable whose probability density function $P_\theta(\theta)$ is related to the number of the crystallized segments N_c. Thus, for a partially crystallized single chain with a given crystal fraction χ, all the possible configurations of the crystallized segments can be taken into account only by considering the probability distribution of the angle θ. As a consequence, the probability density function $P_c(\boldsymbol{r}_c)$ of the crystallized domain is identical with that of the angle θ:

$$P_c(\boldsymbol{r}_c) = P_\theta(\theta). \tag{14}$$

Again, considering the configuration independence between amorphous and crystallized domains, the probability density function of the partially crystallized single chain $P(\boldsymbol{r})$ is derived through the convolution integration $*$ of the amorphous and crystallized probability density functions $P_a(\boldsymbol{r}_a)$ and $P_c(\boldsymbol{r}_c)$:

$$\begin{aligned} P(\boldsymbol{r}) &= P_a(\boldsymbol{r}_a) * P_c(\boldsymbol{r}_c) = \int_{\mathbb{R}^3} P_a(\boldsymbol{r}-\boldsymbol{r}_c)P_c(\boldsymbol{r}_c)d\boldsymbol{r}_c \\ &= \left[\frac{3}{2(1-\chi)\pi N l^2}\right]^{3/2} \int_0^\pi \exp\left\{-(1-\chi)N\Re\left[\frac{1}{1-\chi}\sqrt{\left(\frac{\lambda}{\sqrt{N}}\right)^2+\chi^2-2\frac{\lambda}{\sqrt{N}}\chi\cos\theta}\right]\right\}P_\theta(\theta)d\theta. \end{aligned} \tag{15}$$

Obviously, due to the complexity of the functional form, it is almost impossible to directly obtain a compact expression of the probability density function $P(\boldsymbol{r})$ from Eq. (15), even if an explicit expression of $P_\theta(\theta)$ is given. In order to overcome this difficulty, we introduce a representative angle $\tilde{\theta}$ by considering the basic property of the probability density function $P_\theta(\theta)$, i.e. $\int_0^\pi P_\theta(\theta)d\theta = 1$. Then, Eq. (15) is rewritten as

$$\begin{aligned} P(\boldsymbol{r}) &= \left(\frac{3}{2(1-\chi)\pi N l^2}\right)^{3/2} \exp\left\{-(1-\chi)N\Re\left[\frac{1}{1-\chi}\sqrt{\left(\frac{\lambda}{\sqrt{N}}\right)^2+\chi^2-2\frac{\lambda}{\sqrt{N}}\chi\cos\tilde{\theta}}\right]\right\} \\ &= \left(\frac{3}{2\pi N_a l^2}\right)^{3/2} \exp\left\{-N_a\Re\left(\frac{\tilde{\lambda}_a}{\sqrt{N_a}}\right)\right\}, \end{aligned} \tag{16}$$

in which $\tilde{\lambda}_a$ can be regarded as the representative effective stretch corresponding to the angle $\tilde{\theta}$:

$$\tilde{\lambda}_a = \sqrt{\frac{\lambda^2+\chi^2 N-2\lambda\sqrt{N}\chi\cos\tilde{\theta}}{1-\chi}}. \tag{17}$$

Above all, the molecular configuration of the partially crystallized single chain has been analyzed and calculated by means of some statistical mechanical methods. Especially for the random thermal oscillation of the crystal orientation, the probability density function $P_\theta(\theta)$ is treated by introducing the representative angle $\tilde{\theta}$, which is a nonrandom variable depending on both the stretch λ and the crystal fraction χ:

$$\cos\tilde{\theta} = \Omega(\lambda,\chi). \tag{18}$$

Using the function (18), the evolution of the random crystal orientation can be captured and analyzed during the stretch-induced crystallization process, for which the exact expression will be specified later.

B. Free energy

A key point in the thermodynamic treatment of the partially crystallized single chain is the identification of the physical expression of its free energy. Taking the stretch-free amorphous state as the reference state, a two-step strategy is adopted to derive the free energy as illustrated in Fig. 1. Within the proposed two-step strategy, the description of the first step is very similar to a thermal-induced crystallization and that of the second step is similar to an absolutely mechanical stretching.

1. First step: thermal-induced crystallization

In the first step, the transformation of N_c amorphous segments into crystallized segments is performed on the condition that the ends of the remaining amorphous subparts stay free to

occupy most probable locations. This step can be achieved by applying, in a certain manner, a thermodynamic force driving crystallization, and the free energy change can be given by

$$\Delta\psi_{\mathrm{I}\to\mathrm{II}} = -N_{\mathrm{c}}(\Delta H_{\mathrm{m}} - T\Delta S_{\mathrm{m}}) + U_{\mathrm{s}}, \tag{19}$$

where ΔH_{m} and ΔS_{m} are the enthalpy and entropy changes associated with the fusion of equivalent segments from a perfect crystal. These two material constants are obtained from the thermodynamic equilibrium state between crystallized and melted segments in the stretch-free state, and their ratio $T_{\mathrm{m}}^0 = \Delta H_{\mathrm{m}}/\Delta S_{\mathrm{m}}$ corresponds to a characteristic temperature, namely, the equilibrium melting temperature. This temperature is associated to a critical state in which all crystallites can melt theoretically when heated very slowly. In reality, however, the rubber chains without stretching can maintain the fully amorphous state even in a large temperature range quite lower than T_{m}^0. This phenomenon is usually attributed to the additional requirements of the free energy for the formation of the interface between the crystallite and the surrounding amorphous phase, and for the formation of the crystallite surface. These interfacial free energies are totally considered in our theory by introducing U_{s} in Eq. (19) as a general form. Due to the fact that all the interfacial free energies depend heavily on the crystallite morphology, different crystallization theories can give different expressions for U_{s} [39,40]. In this work, considering the form of the fully extended crystallization, a linear relationship between the surface free energy U_{s} and the crystallized segment number N_{c} is adopted as a specific example to simplify the simulation, i.e., $U_{\mathrm{s}} = u_{\mathrm{s}}N_{\mathrm{c}}$, u_{s} being the proportionality coefficient. Accordingly, Eq. (19) can be rewritten as

$$\Delta\psi_{\mathrm{I}\to\mathrm{II}} = -N_{\mathrm{c}}\Delta H_{\mathrm{m}}\left(1 - \frac{T}{T_{\mathrm{m}}^0}\right) + u_{\mathrm{s}}N_{\mathrm{c}}. \tag{20}$$

Besides, recall that after this step, the amorphous subparts occupy the most probable locations. It means that the end-to-end distance of the amorphous part r_{a} is identically equal to the root mean square value $l\sqrt{N_{\mathrm{a}}}$. Under this constraint condition, the chain configuration after the first step is identified and the corresponding probability density P_{II} can be calculated by degenerating the convolution integration in Eq. (15):

$$P_{\mathrm{II}} = \left(\frac{3}{2\pi N_{\mathrm{a}}l^2}\right)^{3/2} \exp\left\{-N_{\mathrm{a}}\Re\left(\frac{1}{\sqrt{N_{\mathrm{a}}}}\right)\right\}. \tag{21}$$

2. Second step: absolutely mechanical stretching

In the second step, the ends of the partially crystallized chain are dragged to the expected position, the crystal fraction remaining unchanged. Since the crystal is considered as a rigid entity and substantially stiffer than the amorphous part, we assume no stored strain energy during the stretching. The free energy change is fully attributed to the change of the conformational entropy:

$$\Delta\psi_{\mathrm{II}\to\mathrm{III}} = -T(s_{\mathrm{III}} - s_{\mathrm{II}}), \tag{22}$$

where $s_{\mathrm{III}} = k_B \ln(P_{\mathrm{III}})$ and $s_{\mathrm{II}} = k_B \ln(P_{\mathrm{II}})$ are the conformational entropies related to the probability densities $P_{\mathrm{III}} = P(\boldsymbol{r})$ and P_{II}. The term k_B is the Boltzmann's constant.

Substituting Eqs. (16) and (21) into Eq. (22), we can obtain

$$\Delta\psi_{\mathrm{II}\to\mathrm{III}} = k_{\mathrm{B}}TN_{\mathrm{a}}\left\{\Re\left(\frac{\tilde{\lambda}_{\mathrm{a}}}{\sqrt{N_{\mathrm{a}}}}\right) - \Re\left(\frac{1}{\sqrt{N_{\mathrm{a}}}}\right)\right\}, \tag{23}$$

which represents the stored free energy resulting from the change of the representative effective stretch (17) without any chemical energy change.

3. Final expression

The free energy of the partially crystallized chain ψ is identified as the sum of the two previous free energy changes, i.e., $\psi = \Delta\psi_{\mathrm{I}\to\mathrm{II}} + \Delta\psi_{\mathrm{II}\to\mathrm{III}}$. Consequently, it takes the following final expression:

$$\begin{aligned}\psi = &-N_{\mathrm{c}}\Delta H_{\mathrm{m}}\left(1 - \frac{T}{T_{\mathrm{m}}^0}\right) + u_{\mathrm{s}}N_{\mathrm{c}} \\ &+k_{\mathrm{B}}TN_{\mathrm{a}}\left\{\Re\left(\frac{\tilde{\lambda}_{\mathrm{a}}}{\sqrt{N_{\mathrm{a}}}}\right) - \Re\left(\frac{1}{\sqrt{N_{\mathrm{a}}}}\right)\right\}.\end{aligned} \tag{24}$$

It is worth noting that, although the two-step strategy applied for the free energy derivation is hypothetical, it results in a real and accurate physical expression of the free energy. As a thermodynamic potential, the value of the free energy is only dependent on the initial and final states and independent of the thermomechanical history during processing. The original intention of conceiving this two-step strategy is to employ the thermodynamic material parameters coming from the stretch-free equilibrium state and to satisfy the physical consistency.

C. Kinetics

In general, the stretch-induced crystallization is a recoverable micromechanism associated with a dissipative hysteretic response, which can be viewed as an irreversible thermodynamic process accompanied with energy dissipation [41]. In order to exactly describe this process in a single chain, the set of the selected independent state variables[3] includes not only the temperature T and the stretch λ, but also the crystal fraction χ. As an internal state variable, the crystal fraction χ can effectively capture the crystallization-induced microstructural evolution of the single chain, which leads to the history-dependent thermomechanical response at the macroscale. According to the internal state variable theory, the non-negative intrinsic dissipation D during the stretch-induced crystallization process can be expressed as

$$D = \kappa\dot{\chi} \geqslant 0, \tag{25}$$

where $\dot{\chi}$ is the crystallization rate and can be regarded as a generalized thermodynamic flux, and $\kappa = -\partial\psi/\partial\chi$ is a thermodynamic entity conjugated to the crystal fraction χ and can be correspondingly regarded as a generalized thermodynamic force. In line with Eq. (24), the specific expression of the

[3]All the other thermodynamic quantities are regarded as functions of these selected independent state variables and, especially, the free energy function $\psi(T,\lambda,\chi)$ contains all thermodynamic information about the partially crystallized single chain.

thermodynamic force κ can be deduced as

$$\kappa = \underbrace{N\Delta H_{\mathrm{m}}\left(1-\frac{T}{T_{\mathrm{m}}^{0}}\right)}_{\kappa_T} - \underbrace{u_{\mathrm{s}}N}_{\kappa_{\mathrm{S}}} + \underbrace{k_{\mathrm{B}}TN\left\{\mathbb{Z}\left(\alpha,\frac{\tilde{\lambda}_{\mathrm{a}}}{\sqrt{N_{\mathrm{a}}}}\right)-\mathbb{Z}\left(\frac{1}{2\sqrt{N_{\mathrm{a}}}},\frac{1}{\sqrt{N_{\mathrm{a}}}}\right)\right\}}_{\kappa_\lambda}, \quad (26)$$

in which we define $\mathbb{Z}(x,y)$ as a function written as

$$\mathbb{Z}(x,y) = x\mathcal{L}^{-1}(y) + \ln\frac{\mathcal{L}^{-1}(y)}{\sinh\mathcal{L}^{-1}(y)}, \quad (27)$$

and the term α is expressed as

$$\alpha = \frac{\Omega\frac{\lambda}{\sqrt{N}} + \chi\frac{\lambda}{\sqrt{N}}\frac{\partial\Omega}{\partial\chi} - \chi}{\sqrt{\left(\frac{\lambda}{\sqrt{N}}\right)^2 + \chi^2 - 2\chi\Omega\frac{\lambda}{\sqrt{N}}}}. \quad (28)$$

From the (nonequilibrium) thermodynamic viewpoint the partially crystallized single chain tends towards a thermodynamic equilibrium state, which may be considered as a limiting case where all the thermodynamic quantities do not depend upon time. This implies that the internal state variable χ has a tendency to reach a stable value under the prescribed stretch λ, i.e., $\dot{\chi} = 0$. This tendency, characterized by the thermodynamic flux $\dot{\chi}$, can be considered to be driven by the thermodynamic force κ. On the condition that the deviation from the thermodynamic equilibrium state is small and considering that the intrinsic dissipation D must be non-negative, a linear relationship is assumed between the thermodynamic flux $\dot{\chi}$ and the force κ:

$$\dot{\chi} = A\kappa, \quad (29)$$

where A is a positive coefficient.

Moreover, from Eq. (26), we can find that the thermodynamic force κ consists of three parts. The first part, κ_T, is the thermally activated crystallization force correlated to the process activation at temperatures lower than T_{m}^{0} and to the process impedance at temperatures higher than T_{m}^{0}. The second part, κ_S, is the crystallization resistance which is produced by the interface and surface formation and accounts for the delay of crystallization in temperature and stretch. The last and third part, κ_λ, is the stretch-induced crystallization force, which should vanish to zero at the initially fully amorphous state without stretching, $\lambda = 1$ and $\chi = 0$. This initial condition related to the material thermodynamic stability is crucial for the model formulation. It can be satisfied by letting $\cos\tilde{\theta} = \Omega(1,0) = 1/2\sqrt{N}$ in Eq. (18), which may reveal that, for a single chain with sufficiently large length, the crystallite forms initially in a direction nearly perpendicular to the chain axis. However, considering the fact that the newly formed crystal after stretching tends to orient itself towards the chain direction, we formulate the specific dependence of $\tilde{\theta}$ on both λ and χ as follows:

$$\cos\tilde{\theta} = \Omega(\lambda,\chi) = \frac{2\sqrt{N}-1}{2\sqrt{N}(1-e^{-\gamma})}(1-e^{-\gamma\omega}) + \frac{1}{2\sqrt{N}}, \quad (30)$$

where the parameter γ is a coefficient controlling the orientation rate of the newly formed crystal with the chain axis, and

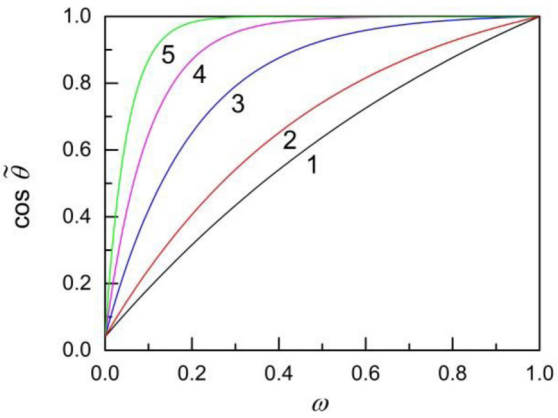

FIG. 2. Crystal orientation with the ω parameter, 1: $\gamma = 1$, 2: $\gamma = 2$, 3: $\gamma = 5$, 4: $\gamma = 10$, 5: $\gamma = 20$.

the variable ω is given by

$$\omega = a\frac{\lambda-1}{\sqrt{N}-1} + b\chi, \quad (31)$$

in which $a \in [0,1]$ and $b \in [0,1]$ are the weight coefficients for the stretch and crystallization effects on the angle $\tilde{\theta}$, respectively, and the sum of them is unit, i.e., $a + b = 1$. Figure 2 presents the $\cos\tilde{\theta}$ evolution with the variable ω in which we can appreciate the γ dependence of the rate in crystal orientation with the chain axis. Although exponential functions are introduced in Eq. (30) to describe the evolution of the crystal orientation, other functional expressions satisfying the requirements could be employed. In the remaining part of the paper, the following values are retained: $a = 0.8$, $b = 0.2$, and $\gamma = 10$.

The normalized force f in the single chain is obtained from the differentiation of the free energy function (24) with respect to the chain stretch,

$$f = \frac{\partial\psi}{\partial\lambda} = k_{\mathrm{B}}TN\beta\mathcal{L}^{-1}\left(\frac{\tilde{\lambda}_{\mathrm{a}}}{\sqrt{N_{\mathrm{a}}}}\right), \quad (32)$$

in which the term β is expressed as

$$\beta = \frac{\frac{\lambda}{N} - \Omega\frac{\chi}{\sqrt{N}} - \chi\frac{\lambda}{\sqrt{N}}\frac{\partial\Omega}{\partial\lambda}}{\sqrt{\left(\frac{\lambda}{\sqrt{N}}\right)^2 + \chi^2 - 2\chi\Omega\frac{\lambda}{\sqrt{N}}}}. \quad (33)$$

The macrokinematic variables are obtained through an averaging over all possible orientations of the microstretch λ. In this procedure, the average number of chains per unit reference volume n is introduced and N becomes the average number of segments in the chain network.

III. MODEL RESULTS AND DISCUSSION

In this section, the main factors governing the crystallinity and the macroresponse are examined using the proposed model under the equilibrium state and the nonequilibrium state involved during stretching and recovery and continuous relaxation. In the bellow discussion, the term λ corresponds to the uniaxial stretch applied at the macrolevel. Several inputs related to microstructural and thermodynamic

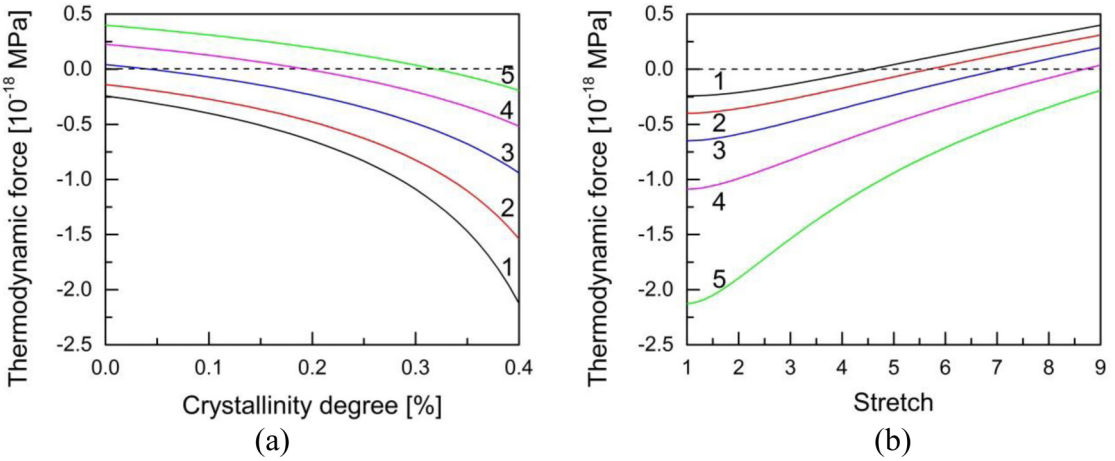

FIG. 3. Thermodynamic force at $T = 20^\circ$ C (a) as a function of crystallinity degree for different stretches, 1: $\lambda = 1$, 2: $\lambda = 3$, 3: $\lambda = 5$, 4: $\lambda = 7$, 5: $\lambda = 9$, and (b) as a function of stretch for different crystallinity degrees, 1: $\chi = 0\%$, 2: $\chi = 10\%$, 3: $\chi = 20\%$, 4: $\chi = 30\%$, 5: $\chi = 40\%$.

properties[4] are required by the following modeling: $nk_BT_0 = 0.06\,\text{MPa}$ $(T_0 = 20\,^\circ\text{C})$, $N = 150$, $A = 5.0 \times 10^{16}\,\text{MPa}^{-1}\,\text{s}^{-1}$, $\Delta H_m = 4400\,\text{J mol}^{-1}$, $T_m^0 = 25\,^\circ\text{C}$, $u_s = 1500\,\text{J mol}^{-1}$.

A. Equilibrium state

Prior to examining the crystallinity evolution, numerical simulations are carried out to address the influence of temperature as well as stretch on the equilibrium crystallization. A key point of our theory is the thermodynamic force κ in Eq. (26) which is a decreasing function of the crystallinity and an increasing function of the stretching. These two opposite evolutions are shown in Fig. 3. Since the thermodynamic force drives the crystallinity evolution by the kinetics law (29), the equilibrium state corresponds to a free thermodynamic force, i.e., $\kappa = 0$. From the experimental viewpoint, the true thermodynamic equilibrium state at a certain temperature T and a certain stretch λ may require a quasi-infinite duration in an isothermal monotonic stretching. In order to overcome this difficulty, two experimental protocols in two steps have been used in the literature [18–20]. The first method consists of a cooling of a sample loaded at constant stretch λ well below a certain temperature T and the quasiequilibrium state can be then reached after progressively warming back up to T. The second method consists of a stretching of a sample at constant temperature T well above a certain stretch λ and the quasiequilibrium state can be then reached after relaxation to λ. However, the equilibrium state obtained by means of the two experimental protocols is usually different, which indicates the great complexity of the history-dependent thermomechanical response during the stretch-induced crystallization process.

[4]It is important to note that nonrealistic values for the melting enthalpy ΔH_m and the melting temperature T_m^0 must be used as inputs of existing constitutive theories in order to obtain correct quantitative comparisons with experiments [24,27–30]. More realistic values are used in this work by introducing in our theory the crystallite surface free energy. A quantitative evaluation of our theory remains, however, an important issue for further studies.

The evolution of the simulated equilibrium state is presented in Fig. 4 as a function of stretch and in Fig. 5 as a function of temperature. The plots in Fig. 4(a) show a quasilinear relationship between the crystallinity degree and the stretch. It can be observed that the higher the temperature, the lower the crystallinity degree and the higher the critical stretch at which the crystallization is nonzero. The critical stretch deduced from Fig. 4(a) is plotted with the corresponding temperature in Fig. 4(b) such that a straight-line fit adequately describes the results. This is a well-known experimental observation [7]. Figure 5 demonstrates that both the crystallinity degree and the stress evolve linearly with temperature but in an opposite manner. This opposite evolution was experimentally highlighted by several authors [7,20]. The stress increase with temperature is due to two concomitant factors, the decrease in crystallinity degree and the increase in entropy stiffness nk_BT of the amorphous domain. That explains why the slope decreases for the two lower stretch levels after a temperature where the crystallization does not take place. Indeed, in the absence of crystallization, the slope only depends on the entropy effect. Interestingly, this difference in slope was experimentally highlighted by Toki *et al.* [14].

B. Nonequilibrium state

The question which arises now is how the above factors could affect the kinetics of crystallization during the course of a stretching followed by a recovery. During these simulations, the stretch λ is ramped to a maximum level λ_{max} and then ramped down to 1. Figures 6–8 provide the stretching and recovery response for different key factors (namely, stretch level λ_{max}, stretch rate $\dot{\lambda}$, and temperature T) governing the micromechanism and the macroresponse. It is satisfactory to point out that the model is able to reproduce the delay in the onset of crystallization by using a simple kinetics law given by Eq. (29) with no additional threshold or restriction. A global view at these plots shows that the stretch-induced crystallization during stretching and the stretch-induced melting during recovery differ, which is the exclusive reason for the observed stress hysteresis. This result reveals that the mechanical hysteresis loop is entirely controlled by the crystallization

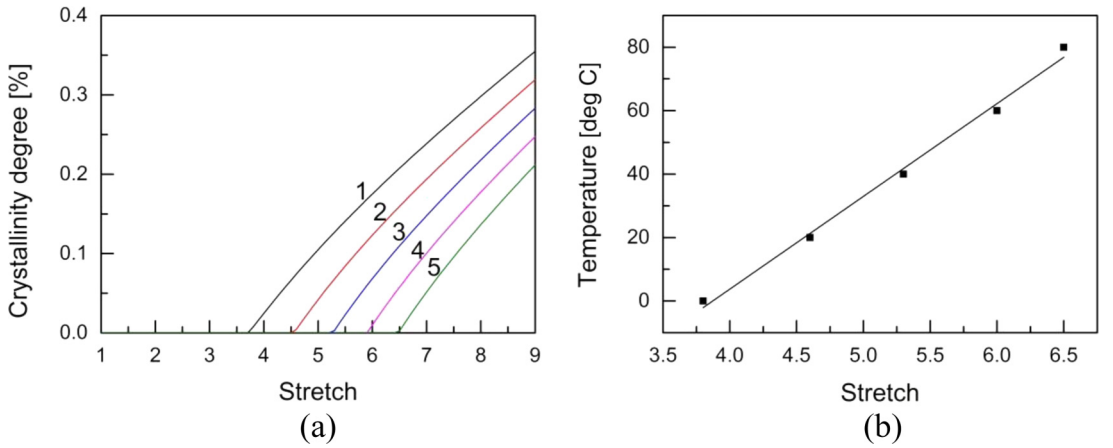

FIG. 4. Equilibrium crystallization: (a) crystallinity vs stretch, (b) temperature vs critical stretch, 1: $T = 0\,^{\circ}\mathrm{C}$, 2: $T = 20\,^{\circ}\mathrm{C}$, 3: $T = 40\,^{\circ}\mathrm{C}$; 4: $T = 60\,^{\circ}\mathrm{C}$, 5: $T = 80\,^{\circ}\mathrm{C}$.

and melting process and is not due to viscous effects of the amorphous rubber network since no viscous component is introduced in our theory, which is in accordance with experimental evidence [5–7]. Actually, all history-dependent thermomechanical features at macroscale or microscale originate from the rate-dependent crystallinity evolution governed by Eq. (29). More specifically, the crystallization rate depends on the thermodynamic crystallization force expressed by Eq. (26). The latter, obtained from the differentiation of the proposed free energy in Eq. (24) with respect to the crystallization, is a function of stretch level and temperature. Furthermore, the fact that the crystallinity degree at a given stretch is higher during unloading than during loading is a feature well described by our theory. By decreasing the effective stretch in Eq. (17) the crystallinity thus induces a stress softening, resulting in the stress difference between the loading path and the unloading path. The stress hysteresis and the crystallization hysteresis can be related from an energetic viewpoint by considering the two scales. At the scale of the micromechanism, the crystallization evolution driven by the thermodynamic force induces a local energy dissipation formulated in Eq. (25). This local thermodynamic dissipation is the exclusive reason for the energy dissipation at the macroscale manifested by the stress hysteresis.

Figure 6 presents the crystallinity evolution and the macroresponse for various maximum stretch levels. If the maximum stretch level is lower than a certain critical stretch [equal to 4.7 at 20 °C as shown in Fig. 4(b)] for the onset of crystallization the response during stretching and recovery coincides with that of the amorphous rubber network, shown by a dashed line in Fig. 6(b). At levels of stretch greater than the crystallization-onset stretch, a hysteretic response is observed whose area increases with the maximum stretch. The crystallinity affects the form of the macroresponse by the appearance of a stress inflection from which the strain hardening decreases. The stress upturn experimentally observed at very large stretches requires accounting for a crystallization-induced stiffening effect since it is not due to the contribution of the remaining amorphous fraction [9]. The same mechanism is responsible for two antagonist phenomena, which render it unique—a softening inducing a stress inflection at moderate stretches and a stiffening inducing a stress upturn at very large stretches. Solely the crystallization-induced softening is accounted for in our theory. As illustrated in Fig. 3(b), the

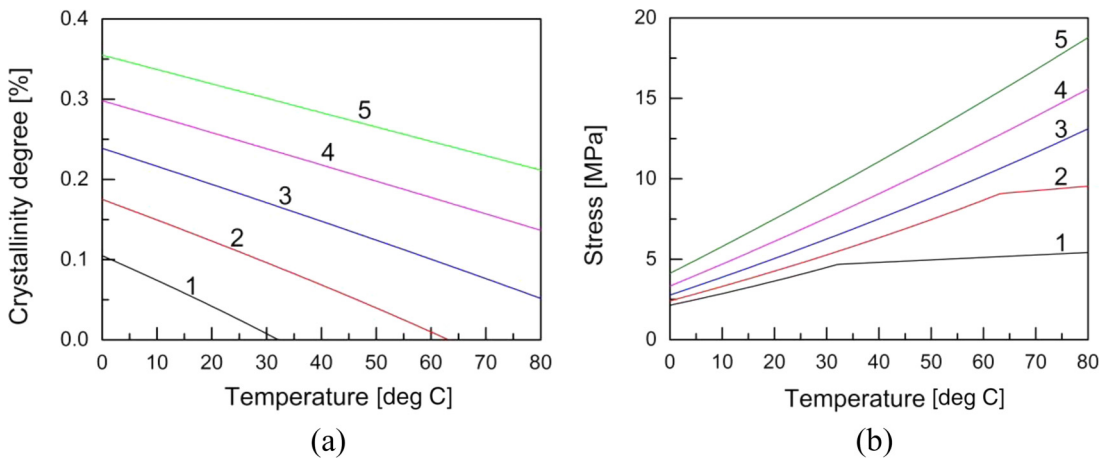

FIG. 5. Equilibrium crystallization: (a) crystallinity vs temperature, (b) stress vs temperature, 1: $\lambda_{max} = 5$, 2: $\lambda_{max} = 6$, 3: $\lambda_{max} = 7$, 4: $\lambda_{max} = 8$, 5: $\lambda_{max} = 9$.

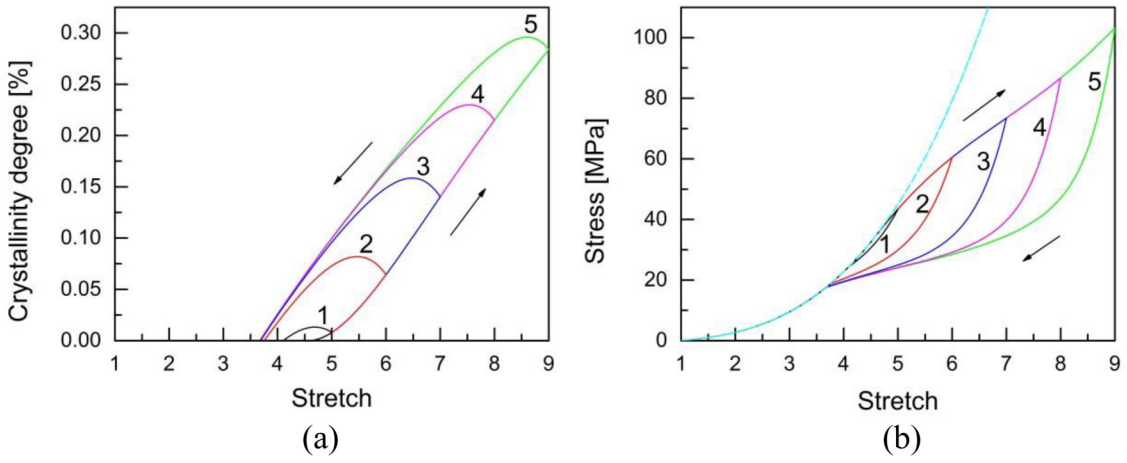

FIG. 6. Stretch-level influence on stretching and recovery: (a) crystallization kinetics, (b) macroresponse, $T = 20\,^{\circ}\mathrm{C}$, $\dot{\lambda} = 0.05/\mathrm{s}$, 1: λ_{max}=5, 2: $\lambda_{max} = 6$, 3: $\lambda_{max} = 7$, 4: $\lambda_{max} = 8$, 5: $\lambda_{max} = 9$.

thermodynamic force given by Eq. (26) increases monotonically with the stretch level. During the course of a stretching, the stretch level increases the crystallinity which consequently decreases the strain hardening. The macroresponse is strongly related to the crystallinity but also to the crystal form. The stiffening could be accounted for by introducing explicitly the crystal form into the molecular configuration of the partially crystallized chain. Consequently, in addition to the crystallinity and the crystal orientation, the effective stretch in Eq. (17) could be reformulated to take into account the crystal form.

Let us now focus on the stretch-rate effects. Remember that no viscous component is introduced in our theory to reproduce any time-dependent feature. Figure 7(a) shows a strong influence of the stretch rate on the crystallinity evolution. The crystallization hysteresis loop area gets smaller and the crystallinity degree increases with decreasing stretch rate. This feature was already experimentally highlighted in [10,12,13]. The rate dependency of the stretch-induced crystallization is a consequence of the time dependency of the crystallization kinetics driven by the thermodynamic force given in Eq. (26). A large stretch rate leads to less time for crystallization and melting, and vice versa. The stretch at complete melting is also found sensitive to the stretch rate whereas the onset of crystallization is found independent of that. A stretch-rate dependence of the nucleation may be predicted by introducing a time-dependent effect into the energy barrier. In addition, the stretch-rate dependency of the stretch-induced material transformation leads to the rate-dependent stress response observed in Fig. 7(b). Indeed, it can be seen that both the amount of stress hysteresis loop area and the magnitude of strain hardening decrease with decreasing stretch rate. If the stretch rate tends to an infinitesimal value the stretch-induced crystallization appears in the form of an equilibrium state and no difference between crystallization and melting happens; that is to say, no mechanical hysteresis is observed. This response is provided in dashed lines in Fig. 7. This is again a confirmation that the crystallization and melting process is the source of the stress hysteresis and more generally of all history-dependent thermomechanical features.

It is now interesting to focus on the temperature effects during stretching and recovery. Figure 8 presents the crystallinity evolution and the macroresponse for various temperatures. It can be observed that there is a regular decrease

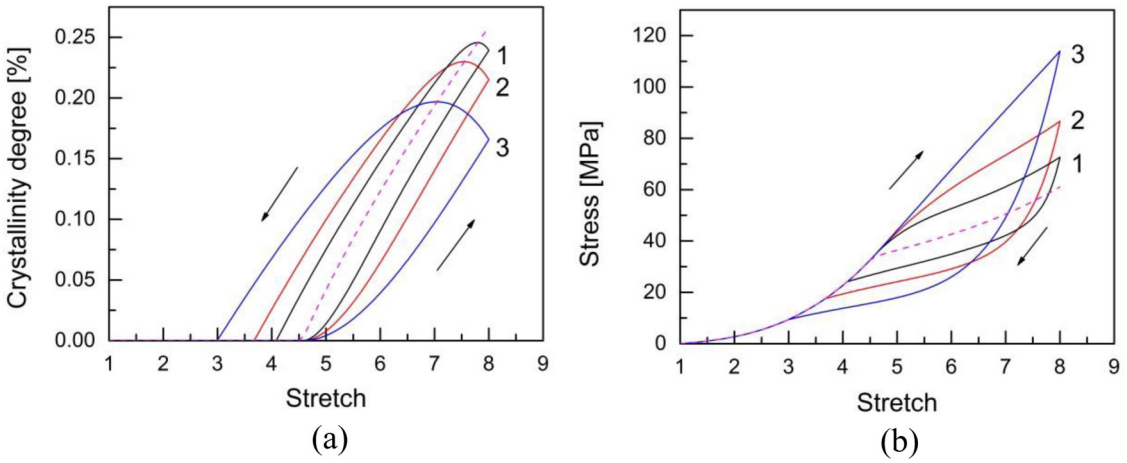

FIG. 7. Stretch-rate influence on stretching and recovery: (a) crystallization kinetics, (b) macroresponse, $T = 20\,^{\circ}\mathrm{C}$, 1: $\dot{\lambda} = 0.025/\mathrm{s}$, 2: $\dot{\lambda} = 0.05/\mathrm{s}$, 3: $\dot{\lambda} = 0.1/\mathrm{s}$, $\lambda_{max} = 8$.

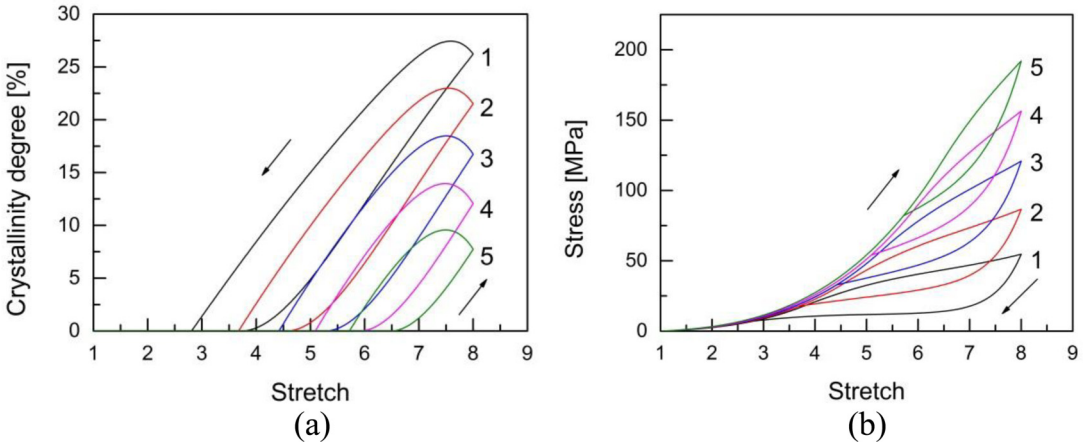

FIG. 8. Temperature influence on stretching and recovery: (a) crystallization kinetics, (b) macroresponse, 1: $T = 0\,^{\circ}\mathrm{C}$, 2: $T = 20\,^{\circ}\mathrm{C}$, 3: $T = 40\,^{\circ}\mathrm{C}$; 4: $T = 60\,^{\circ}\mathrm{C}$, 5: $T = 80\,^{\circ}\mathrm{C}$, $\dot{\lambda} = 0.05/\mathrm{s}$, $\lambda_{\max} = 8$.

of the crystal content with temperature which is consistent with experimental observations [8,10,11]. The temperature effect on the macrostress implies numerous phenomena yet misunderstood in the literature, resulting in a high difference in strain-hardening ability due to chain stretching. Basically, the temperature affects the macroresponse by the entropy effect of the amorphous domain. This phenomenon is concomitant with an increase in crystallinity degree by decreasing the temperature, as a consequence of the temperature dependency of the thermodynamic force given in Eq. (26). Recall that solely the crystallization-induced softening is introduced in our theory via the effective stretch expressed in Eq. (17). Therefore, both phenomena contribute to an increase in stress with temperature. Furthermore, both the onset of crystallization and the completion of melting are strongly affected by the temperature, and increase regularly. The delay $\Delta T = T_{\mathrm{m}} - T_{\mathrm{c}}$ in crystallization is typically termed supercooling under temperature-induced crystallization. The melting temperature T_{m} is usually considered as a thermodynamic property whereas the crystallization temperature T_{c} is not, since it depends on the experimental conditions, in particular on the cooling rate. The origin of the supercooling comes from the energy barrier to the surface formation of crystallites, which depends on the crystallite form and dimension, both being sensitive to the loading conditions. Under isothermal stretch-induced crystallization, the crystallites completely melt at a lower stretch than that at which crystallization starts. This delay $\Delta\lambda = \lambda_{\mathrm{m}} - \lambda_{\mathrm{c}}$ in crystallization can be seen as a superstretching phenomenon as named by Candau *et al.* [40]. The stretch data for the onset of crystallization λ_{c} and the completion of melting λ_{m} extracted from Fig. 8(a) are plotted in Fig. 9 such that two nearly parallel straight-line fits appear and illustrate these two phenomena. This temperature dependence of crystallization and melting is consistent with the experimental observations of Albouy *et al.* [8].

As a final point of discussion, we propose to examine the crystallization response under continuous relaxation. These simulations consist firstly to apply a stretching up to a predetermined level under constant stretch rate and secondly to keep constant this stretch for a prescribed delay during which the evolutions in crystallinity and in stress are computed. The stretching is performed at a sufficiently high rate to limit the crystallization before relaxation. As shown in Figs. 10(a) and 11(a), the crystallization during relaxation starts to increase linearly with the time but it rapidly exhibits a curved profile and tends towards a stabilized state for which there is no change in crystallinity. The reached maximum crystallinity degree corresponds to the equilibrium state plotted in Figs. 4(a) and 5(a). This crystallization evolution process, corresponding to the course of the thermodynamic state from nonequilibrium to equilibrium, is driven in our theory by the thermodynamic force given by Eq. (26). The latter decreases monotonically with crystallinity degree as shown in Fig. 3(a). Recently, Bruning *et al.* [16] measured the crystallinity evolution under continuous relaxation for different stretch levels and temperatures, but without providing the stress evolution. Our simulations in Figs. 10(a) and 11(a) give similar tendencies. More recently, Xie *et al.* [17] measured the stretch-level and temperature dependencies of the continuous stress relaxation as a signature of the crystallinity evolution in a crystallizing rubber, but without definitely providing the crystallinity degree. The authors reported the same trends as those observed in Figs. 10(b)

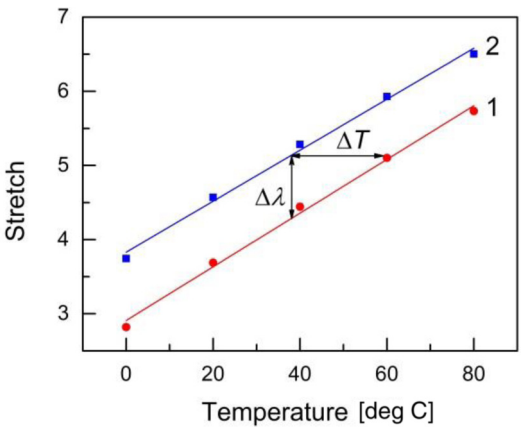

FIG. 9. Supercooling ΔT and superstretching $\Delta\lambda$ phenomena deduced from Fig. 8; 1: onset of crystallization, 2: completion of melting.

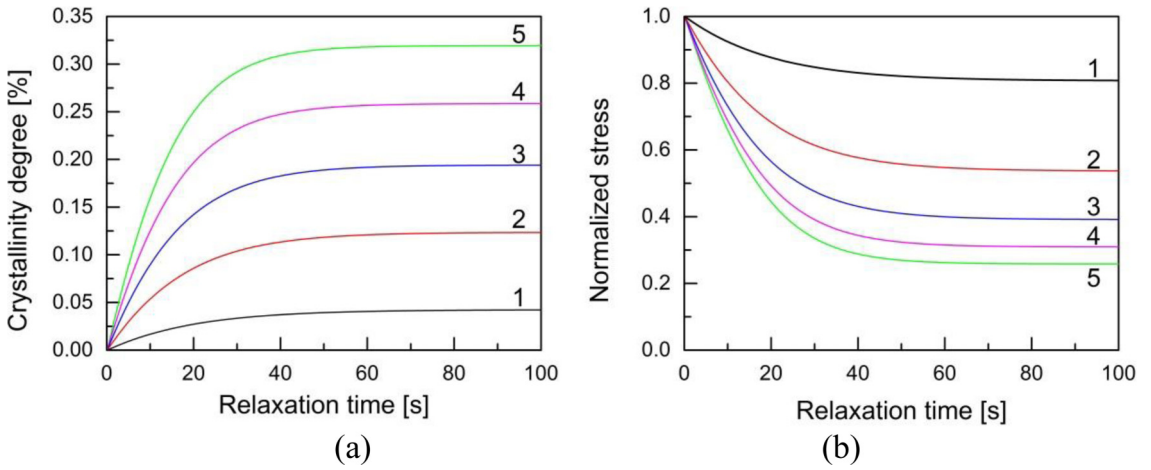

FIG. 10. Stretch-level influence on continuous relaxation: (a) crystallization kinetics, (b) macroresponse, $T = 20\,^{\circ}$C, 1: $\lambda_{max} = 5$, 2: $\lambda_{max} = 6$, 3: $\lambda_{max} = 7$, 4: $\lambda_{max} = 8$, 5: $\lambda_{max} = 9$.

and 11(b). As for the stress hysteresis for which the viscous effects of the amorphous rubber network must be not invoked, according to our simulations the stress relaxation is believed to be solely controlled by the crystallization process under relaxation. Quite interestingly, the normalization of the stress with its maximum value points out a nonlinearity of the stretch-level and temperature effects.

C. Discussion

Our theory provides significant physical insights about a fascinating phenomenon still misunderstood and involves very few physically interpretable material constants: two chain-scale constants, one crystallinity kinetics constant, three thermodynamic constants related to the newly formed crystallites, and a function controlling the crystal orientation with respect to the chain. The complex history-dependent thermomechanical response of natural rubbers necessitates providing a set of formulas, not to increase the flexibility of the resulting model but with the aim to describe the entire set of phenomena in connection to the real system. Our theory, based on a micromechanism inspired molecular chain approach, formulated within the context of the thermodynamic framework, requires a few assumptions, e.g., rotational joints of amorphous segments, full extension of crystallized segments, and proportionality of surface free energy. In spite of these assumptions, our model provides significant insights about the relationship between the micromechanism of crystallization in stretched rubbers and the history-dependent thermomechanical response at the macroscale. The satisfactory simulation results provided by our theory can be attributed to its solid physical foundation. More specifically, the molecular configuration of the partially crystallized chain is objectively analyzed and reasonably described by means of some statistical mechanical methods, especially considering the random thermal oscillation of the crystal orientation. The present theory treats the stretch-induced crystallization as an irreversible thermodynamic process driven by a thermodynamic crystallization force induced by the nonequilibrium thermodynamic state. A realistic physical expression of the chain free energy is derived according to a two-step strategy by separating crystallization and stretching. This strategy can ensure that the theory satisfies a crucial physical condition

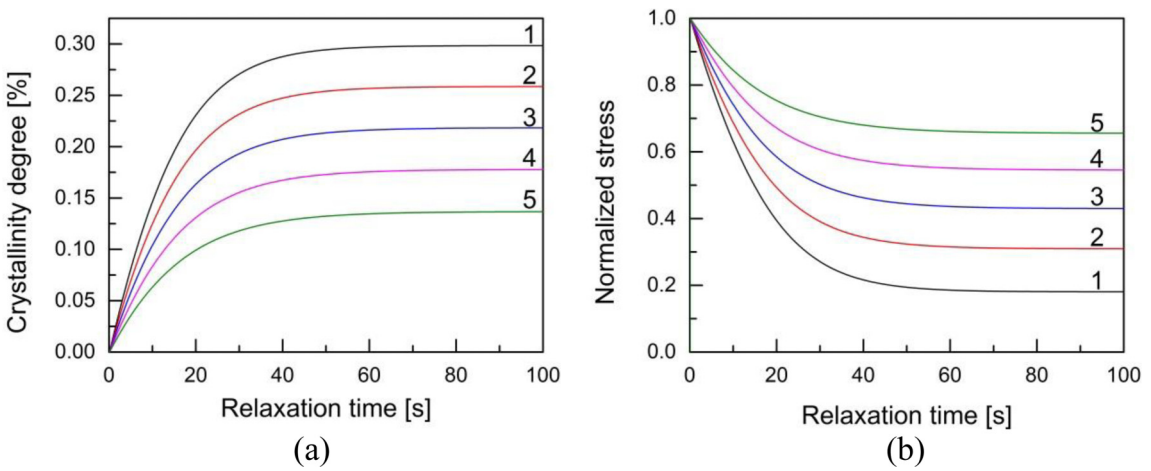

FIG. 11. Temperature influence on continuous relaxation: (a) crystallization kinetics, (b) macroresponse, 1: $T = 0\,^{\circ}$C, 2: $T = 20\,^{\circ}$C, 3: $T = 40\,^{\circ}$C; 3: $T = 60\,^{\circ}$C, 4: $T = 80\,^{\circ}$C, $\lambda_{max} = 8$.

related to the material thermodynamic stability; that is, the thermodynamic crystallization force is null at the initial state under the melting temperature. This is a key point that earlier Flory [27] pointed out as a weakness of his theory, and to date only Mistry and Govindjee [24] try to solve this issue by introducing a "phenomenological" yieldlike function in their theory. This key point is treated from a physical viewpoint in our theory.

More work is, however, needed to introduce into our theory the microstructure of crystallites and their evolution. In particular, in addition to the crystal fraction and orientation, it is believed that the crystallite morphology, in terms of form[5] and size, could also control the thermomechanical macroresponse. It is a way to account for, in our theory, the crystallization-induced stiffening. Moreover, a morphology dependence of the surface free energy would be interesting to establish in order to propose a more realistic onset of crystallization, in particular in terms of rate dependency which can be also viewed as a rate dependency of the necessary supercooling or superstretching. This effect has been experimentally highlighted recently by Candau *et al.* [13]. Also, we must recognize that the crystallization kinetics, inherently dominated by the formula (29) that we have proposed to relate the thermodynamic force and the crystallization rate, is too simple to represent the complex phenomenon. The kinetics law would consider at least (i) a nonlinear relationship that introduces an increase in crystallization resistance during the stretch-induced crystallization, (ii) a difference between the crystallization path during stretching and the melting path during recovery, and (iii) an explicit temperature dependency. Further work is needed to incorporate these important ideas in a comprehensive constitutive theory.

[5]In Anoukou *et al.* [42] the incidence of the crystal form on the stiffening has been studied by means of the concepts of micromechanical homogenization without molecular configuration. It would be interesting to consider this aspect in the present theory in our future works.

IV. CONCLUDING REMARKS

In this work, we present a new micromechanism inspired molecular chain model to describe the thermodynamics and mechanics of stretch-induced crystallization in rubbers. Key factors governing the phenomenon were investigated to better understand the relation between the micromechanism and the macroresponse under the equilibrium state and the nonequilibrium state involved during stretching and recovery, and continuous relaxation. The proposed approach contains very few physically interpretable material constants and seems to be sufficiently rich to provide important indications concerning this fascinating phenomenon.

A quantitative evaluation of our approach remains, however, an important issue for further studies. Furthermore, the capability of our approach needs to be further verified under more complex loading conditions. Especially, the coupling between stored/dissipated energy and material transformation during cycling loading could be investigated using the constitutive theory that we have proposed in a recent work [43,44]. Moreover, as introduced in the Discussion section, our approach, although quite sophisticated, needs improvement for a fully realistic description of the microstructure, such as size and form of crystallites, and its evolution.

[1] J. R. Katz, Rontgenspektrographische untersuchungen am gedehnten kautschuk und ihre mogliche bedeutung fur das problem der dehnungseigenschaften dieser substanz, Naturwissenschaften **13**, 410 (1925).

[2] G. R. Hamed, H. J. Kim, and A. N. Gent, Cut growth in vulcanizates of natural rubber, cis-polybutadiene, and a 50/50 blend during single and repeated extension, Rubber Chem. Tech. **69**, 807 (1996).

[3] W. V. Mars and A. Fatemi, Observations of the constitutive response and characterization of filled natural rubber under monotonic and cyclic multiaxial stress states, J. Eng. Mater. Tech. **126**, 19 (2004).

[4] J. B. Le Cam and E. Toussaint, Volume variation in stretched natural rubber: Competition between cavitation and stress-induced crystallization, Macromolecules (Washington, DC, US) **41**, 7579 (2008).

[5] G. L. Clark, M. Kabler, E. Blanker, and J. M. Ball, Hysteresis in crystallization of stretched vulcanized rubber from x-ray data: Correlation with stress-strain behavior and resilience, Ind. Eng. Chem. **32**, 1474 (1940).

[6] S. Murakami, K. Senoo, S. Toki, and S. Kohjiya, Structural development of natural rubber during uniaxial stretching by in situ wide angle x-ray diffraction using a synchrotron radiation, Polymer **43**, 2117 (2002).

[7] S. Trabelsi, P. A. Albouy, and J. Rault, Crystallization and melting processes in vulcanized stretched natural rubber, Macromolecules (Washington, DC, US) **36**, 7624 (2003).

[8] P. A. Albouy, J. Marchal, and J. Rault, Chain orientation in natural rubber. I. The inverse yielding effect, Eur. Phys. J. E **17**, 247 (2005).

[9] P. A. Albouy, A. Vieyres, R. Perez-Aparicio, O. Sanseau, and P. Sotta, The impact of strain-induced crystallization on strain during mechanical cycling of cross-linked natural rubber, Polymer **55**, 4022 (2014).

[10] J. Rault, J. Marchal, P. Judeinstein, and P. A. Albouy, Chain orientation in natural rubber. II. ^{2}H-NMR study, Eur. Phys. J. E **21**, 243 (2006).

[11] J. Rault, J. Marchal, P. Judeinstein, and P. A. Albouy, Stress-induced crystallization and reinforcement in filled natural rubbers: ^{2}H NMR study, Macromolecules (Washington, DC, US) **39**, 8356 (2006).

[12] N. Candau, L. Chazeau, J. M. Chenal, C. Gauthier, J. Ferreira, E. Munch, and D. Thiaudière, Strain induced crystallization and melting of natural rubber during dynamic cycles, Phys. Chem. Chem. Phys. **17**, 15331 (2015).

[13] N. Candau, R. Laghmach, L. Chazeau, J. M. Chenal, C. Gauthier, T. Biben, and E. Munch, Influence of strain rate and temperature

on the onset of strain induced crystallization in natural rubber, Eur. Polym. J. **64**, 244 (2015).

[14] S. Toki, I. Sics, B. S. Hsiao, M. Tosaka, S. Poompradub, Y. Ikeda, and S. Kohjiya, Probing the nature of strain-induced crystallization in polyisoprene rubber by combined thermomechanical and in situ x-ray diffraction techniques, Macromolecules (Washington, DC, US) **38**, 7064 (2005).

[15] M. Tosaka, K. Senoo, K. Sato, M. Noda, and N. Ohta, Detection of fast and slow crystallization processes in instantaneously-strained samples of cis-1,4-polyisoprene, Polymer **53**, 864 (2012).

[16] K. Bruning, K. Schneider, S. V. Roth, and G. Heinrich, Kinetics of strain-induced crystallization in natural rubber: A diffusion-controlled rate law, Polymer **72**, 52 (2015).

[17] Z. Xie, G. Sebald, and D. Guyomar, Temperature dependence of the elastocaloric effect in natural rubber, Phys. Lett. A **381**, 2112 (2017).

[18] B. Huneau, Strain-induced crystallization of natural rubber: A review of x-ray diffraction investigations, Rubber Chem. Tech. **84**, 425 (2011).

[19] S. Toki, The effect of strain-induced crystallization (SIC) on the physical properties of natural rubber (NR), in *Chemistry, Manufacture and Applications of Natural Rubber*, edited by S. Kohjiya and Y. Ikeda (WoodHead/Elsevier, Cambridge, 2014).

[20] P. A. Albouy and P. Sotta, Strain-induced crystallization in natural rubber, Adv. Polym. Sci. **277**, 167 (2017).

[21] M. Kroon, A constitutive model for strain-crystallising rubber-like materials, Mech. Mater. **42**, 873 (2010).

[22] R. Dargazany, V. N. Khiem, and M. Itskov, A generalized network decomposition model for the quasi-static inelastic behavior of filled elastomers, Int. J. Plast. **63**, 94 (2014).

[23] R. Dargazany, V. N. Khiem, E. A. Poshtan, and M. Itskov, Constitutive modeling of strain-induced crystallization in filled rubbers, Phys. Rev. E **89**, 022604 (2014).

[24] S. J. Mistry and S. Govindjee, A micro-mechanically based continuum model for strain-induced crystallization in natural rubber, Int. J. Solids Struct. **51**, 530 (2014).

[25] J. Guilie, L. Thien-Nga, and P. Le Tallec, Micro-sphere model for strain-induced crystallisation and three-dimensional applications, J. Mech. Phys. Solids **81**, 58 (2015).

[26] R. Rastak and C. Linder, A non-affine micro-macro approach to strain-crystallizing rubber-like materials, J. Mech. Phys. Solids **111**, 67 (2018).

[27] P. J. Flory, Thermodynamics of crystallization in high polymers. I. Crystallization induced by stretching, J. Chem. Phys. **15**, 397 (1947).

[28] P. J. Flory, Thermodynamics of crystallization in high polymers. IV. A theory of crystalline states and fusion in polymers, copolymers, and their mixtures with diluents, J. Chem. Phys. **17**, 223 (1949).

[29] J. J. Arlman and J. M. Goppel, On the degree of crystallinity in natural rubber, Appl. Sci. Res. **2**, 1 (1951).

[30] Z. Xie, C. Wei, D. Guyomar, and G. Sebald, Validity of Flory's model for describing equilibrium strain-induced crystallization (SIC) and thermal behavior in natural rubber, Polymer **103**, 41 (2016).

[31] R. J. Roe, K. J. Smith, Jr., and W. R. Krigbaum, Equilibrium degrees of crystallization predicted for "single pass" and folded chain crystallite models, J. Chem. Phys. **35**, 1306 (1961).

[32] R. J. Gaylord, A theory of the stress-induced crystallization of crosslinked polymeric networks, J. Polym. Sci., Part B: Polym. Phys. **14**, 1827 (1976).

[33] R. J. Gaylord and D. J. Lohse, Morphological changes during oriented polymer crystallization, Polym. Eng. Sci. **16**, 163 (1976).

[34] K. J. Smith, Crystallization of networks under stress, Polym. Eng. Sci. **16**, 168 (1976).

[35] M. Avrami, Kinetics of phase change. I. General theory, J. Chem. Phys. **7**, 1103 (1939).

[36] M. Avrami, Kinetics of phase change. II. Transformation-time relations for random distribution of nuclei, J. Chem. Phys. **8**, 212 (1940).

[37] M. Avrami, Granulation, phase change, and microstructure. III. Kinetics of phase change, J. Chem. Phys. **9**, 177 (1941).

[38] M. C. Wang and E. Guth, Statistical theory of networks of non-Gaussian flexible chains, J. Chem. Phys. **20**, 1144 (1952).

[39] O. Dolynchuk, I. Kolesov, R. Androsch, and H. J. Radusch, Kinetics and dynamics of two-way shape-memory behavior of crosslinked linear high-density and short-chain branched polyethylenes with regard to crystal orientation, Polymer **79**, 146 (2015).

[40] N. Candau, R. Laghmach, L. Chazeau, J. M. Chenal, C. Gauthier, T. Biben, and E. Munch, Strain-induced crystallization of natural rubber and cross-link densities heterogeneities, Macromolecules (Washington, DC, US) **47**, 5815 (2014).

[41] Q. Guo, F. Zaïri, H. Baraket, M. Chaabane, and X. Guo, Pre-stretch dependency of the cyclic dissipation in carbon-filled SBR, Eur. Polym. J. **96**, 145 (2017).

[42] K. Anoukou, F. Zaïri, M. Naït-Abdelaziz, A. Zaoui, Z. Qu, J. M. Gloaguen, and J. M. Lefebvre, A micromechanical model taking into account the contribution of α- and γ-crystalline phases in the stiffening of polyamide 6-clay nanocomposites: A closed-formulation including the crystal symmetry, Composites, Part B **64**, 84 (2014).

[43] Q. Guo, F. Zaïri, and X. Guo, A thermo-viscoelastic-damage constitutive model for cyclically loaded rubbers. Part I: Model formulation and numerical examples, Int. J. Plast. **101**, 106 (2018).

[44] Q. Guo, F. Zaïri, and X. Guo, A thermo-viscoelastic-damage constitutive model for cyclically loaded rubbers. Part II: Experimental studies and parameter identification, Int. J. Plast. **101**, 58 (2018).